(Co-)Oligomerization of Olefins to Hydrocarbon Fuels: Influence of Feed Composition and Pressure

Constantin Fuchs, Ulrich Arnold*, and Jörg Sauer

The co-oligomerization of methanol-based C_{2-4} olefins on a heterogeneous nickel silica-alumina catalyst enables the production of fuel-range hydrocarbons. The objective of this study was the production of gasoline and jet fuel, which was achieved with an overall selectivity of above 90 %. The influence of olefin feed composition and pressure was investigated at 120 °C. By employing olefin mixtures instead of one single olefin, selectivity to specific chain lengths decreases and quantities of the individual products converge. An increase of olefin pressure from 16 to 32 bar slightly shifts the liquid products to shorter oligomers and raises feed conversion.

Keywords: Heterogeneous catalysis, Methanol, Olefins, Oligomerization, Renewable fuels

Received: November 22, 2022; *revised:* February 07, 2023; *accepted:* March 02, 2023

1 Introduction

Sustainable methanol is gaining more and more importance in terms of energy transition and the production of renewable fuels and chemicals [1]. The conversion of methanol to C_{2-4} olefins (MTO) with subsequent oligomerization to hydrocarbons in the range of gasoline and jet fuel represents a promising possibility for continued operation of existing fleets in the entire transportation sector [2]. Dimethyl ether (DME), synthesized by dehydration of methanol, is also an option for olefin supply via the DME-to-Olefins process (DTO) [3, 4]. Fig. 1 illustrates the complete process chain starting with MTO or DTO conversion, followed by olefin oligomerization and finally, hydrogenation of the resulting higher olefins to paraffinic fuels, which are usable in the existing distribution and tank infrastructure.

The produced paraffinic fuels do not contain any aromatics. Since aromatics are precursors for the formation of particulate matter during engine combustion, particle formation and emission can be significantly reduced by avoiding them. On the other hand, aromatics contribute significantly to a high fuel performance, e.g., in terms of high octane numbers and densities [5]. Especially for gasoline, these properties are important to meet the corresponding standard DIN EN 228 [6]. To compensate for the absence of aromatics, paraffinic fuels for spark-ignition engines should exhibit a high molecular branching such as the prototypic 2,2,4-trimethylpentane with an octane number of 100 [7], also known as iso-octane. The heterogeneously catalyzed co-oligomerization offers a suitable pathway for producing such hydrocarbons in the range of gasoline and jet fuel by coupling olefin monomers. As feedstocks, particularly ethylene, propylene and butylenes are considered, which

are the main components of a typical MTO product mixture [8–10]. Conversion of these olefins is outlined in Fig. 2, to give only a few examples of possible oligomers.

The oligomerization of ethylene has been widely studied [11–13]. At temperatures below 250 °C, ethylene inevitably requires transition metals as catalysts, e.g., nickel supported on silica-alumina [13]. On such metal sites, ethylene starts the carbon chain growth via a coordination-insertion mechanism [11]. In contrast, higher olefins like propylene or butylenes can form secondary or tertiary carbenium ions at Brønsted acid sites enabling the chain growth [14–16]. Consequently, Brønsted acid sites are crucial for catalytic activity and transition metals are not required [17]. In general, research on oligomerization reactions mostly focuses on the preparation of linear molecules, e.g., for synthetic lubricants, and often, homogeneous metal catalysts or ionic salts are employed [18–22]. Concerning heterogeneous catalysts, in particular zeolites such as ZSM-5 are employed [23–26]. Furthermore, ion exchange resins, metal-organic frameworks and amorphous, mesoporous silica-alumina support materials were investigated [14, 17, 27–30]. Microporous zeolites rapidly deactivate by pore blockage caused by the formation of higher oligomers on Brønsted sites [31]. The mesoporous silica-aluminas are more attractive due to their high activity and particularly long-term stability [11]. Additionally, the amount of Lewis and Brønsted sites of

[1]Constantin Fuchs, [1]Dr. Ulrich Arnold
(ulrich.arnold@kit.edu), [1]Prof. Dr.-Ing. Jörg Sauer
[1]Karlsruhe Institute of Technology, Institute of Catalysis Research and Technology, Hermann-von-Helmholtz-Platz 1, 76344 Eggenstein-Leopoldshafen, Germany.
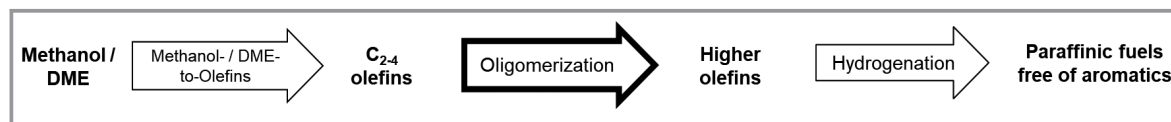
Figure 1. Process chain for the production of paraffinic fuels from methanol/DME via olefin oligomerization.
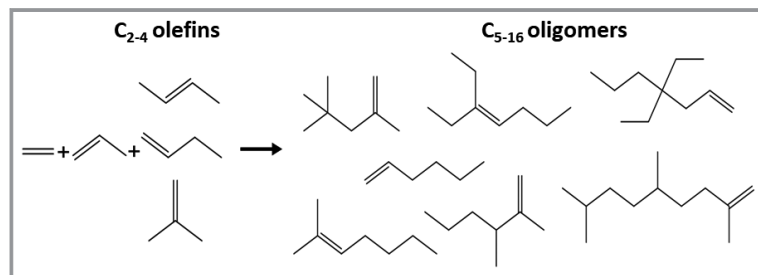

Figure 2. Examples for the co-oligomerization of ethylene, propylene and butylenes to fuel range oligomers.

silica-aluminas is easily tunable by variation of the silica content, while the strength of the Brønsted sites is comparable to zeolites [32]. Consequently, mildly acidic catalysts are beneficial to avoid coking and catalyst deactivation by formation of higher oligomers.

The influence of different reaction conditions like temperature or space velocity was also studied as well as the role of different catalysts [12, 13, 15, 16, 26, 33]. Temperature and space velocity showed an unambiguous behavior regarding their influence on the product mixture, whereas contradictory effects were reported for pressure variations. A trend towards higher oligomers with increasing olefin partial pressure on zeolites and mesoporous silica-aluminas was shown, e.g., by Koninckx et al. [12], Betz et al. [13] and Jan et al. [34]. In contrast, Silva et al. and Díaz et al. observed the opposite behavior, namely a shift to smaller oligomers with increasing pressure, in the case of HZSM-5, BEA and aluminosilicates [26, 35, 36].

However, most of the work concentrated on the oligomerization of only one olefin species and the heterogeneously catalyzed co-oligomerization of olefin mixtures has been sparsely considered. As an example from industry, the Catpoly process, developed by UOP in the 1930s, uses solid phosphoric acid to convert C_{3+4} olefins to gasoline with chain lengths in the range of C_{6-10} [37, 38]. Another example is the Mobil Olefins to Gasoline and Distillate (MOGD) process, developed by Mobil during the oil crises in the 1970s, for the conversion of C_{2+3+4} olefin mixtures on zeolite ZSM-5 [24, 39]. Nevertheless, none of the processes is currently in operation on an industrial scale for reasons of economy. In current literature, fuel-relevant properties are not considered, as the focus is on producing linear molecules with homogeneous catalysts [18, 25]. Thus, further development in the field of co-oligomerization of C_{2-4} olefins to standard-compliant fuels has been rather neglected since the 1980s.

This study focuses on the targeted synthesis of high-octane gasoline and jet fuel via heterogeneously catalyzed oligomerization of ethylene, propylene and 1-butylene with nickel supported on a mildly acidic mesoporous silica-alumina. In the following, the effect of different olefin feed compositions is described, regarding product distribution and degree of branching. Additionally, different olefin partial pressures of olefin feed mixtures, namely 16 and 32 bar, were investigated to gain insights into the reaction mechanisms and possibilities of tuning the composition of the product mixture.

2 Material and Methods

As catalyst, nickel supported on a commercial silica-alumina (SIRALOX 40 from Sasol) has been applied. The mesoporous support has been impregnated with a nickel salt solution by incipient wetness impregnation until loading reached 5 wt % of nickel. For this purpose, the support was first calcined at 550 °C for 8 h before the nickel salt solution was added. This solution was prepared from $Ni(NO_3)_2 \cdot 6 H_2O$ (99.9 %, ABCR) and distilled water. After subsequent drying at 50 °C, the catalyst precursor was calcined again at 550 °C. Finally, the catalyst powder was classified by pelletizing and subsequent crushing to a particle size of 250–500 μm. Surface properties of the catalyst measured by nitrogen sorption isotherms at 77 K with a Novatouch 4LX analyzer (Quantachrome Instruments), are shown in Tab. 1. The Brunauer-Emmett-Teller (BET) method in the relative pressure (p/p_0) range from 0.002 to 0.3 was applied for calculating the specific surface area. The Barrett-Joyner-Halenda (BJH) method was utilized for the determination of the total pore volume and the average pore diameter. The acidity was analyzed by NH_3-TPD analysis using an AutoChem 2950 HP (Micromeritics). The results for the SIRALOX 40 support and the impregnated catalyst with 5 wt % nickel are

Table 1. Properties of SIRALOX 40 with 5 wt % Ni loading.

Catalyst property	SIRALOX 40 with 5 wt % Ni
Al_2O_3 / SiO_2	60 / 40
Pore volume V_{Pore} [mL g^{-1}]	1.22
Pore diameter d_{Pore} [nm]	8.0
BET surface S_{BET} [m^{2}g^{-1}]	357

depicted in Fig. 3. The nickel-loaded catalyst reveals a higher acidity than the blank support due to the additional Lewis acid sites provided by nickel. Further information on the catalyst can be found in [13] and [40].
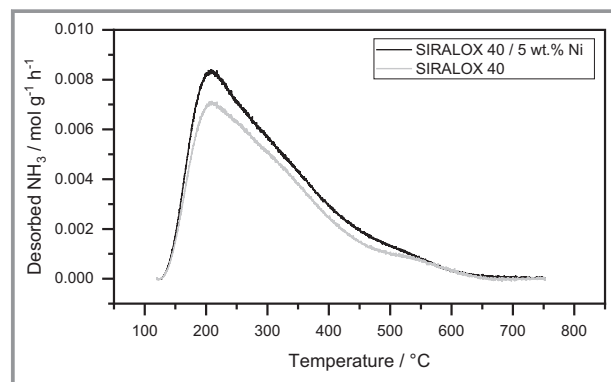

Figure 3. NH$_3$-TPD analysis for SIRALOX 40 and the impregnated catalyst with 5 wt % nickel.

With this catalyst, experiments in a lab-scale plant with different feedstocks and olefin partial pressures have been carried out. The laboratory system contains a continuously operating plug-flow reactor as already described by Betz et al. [13]. It was originally designed for ethylene (99.9 %, Air Liquide) oligomerization and afterwards extended by a co-feeding system [27] for liquid propylene (99.5 %, Air Liquide) and 1-butylene (99.4 %, Air Liquide). The liquified gases are cooled continuously to remain liquid before being compressed to reaction pressure by HPLC pumps (Wagner), controlled by Coriolis mass flow meters (Bronkhorst). In each experiment, 5 g of fresh catalyst were used. Regarding the operating conditions, a previous study [13] showed that for the applied catalyst a mild temperature of 120 °C is beneficial concerning olefin conversion, selectivity to octenes, and their degree of branching. Accordingly, in all experiments, 120 °C and a weight hourly space velocity (*WHSV*) of 4 h^{-1} were applied. The gaseous phase was analyzed by an online gas chromatograph (HP 5890 with Rt-Alumina BOND/Na$_2$SO$_4$ column). The condensed liquid products were analyzed with an offline gas chromatograph (Agilent 6890 with DB-1 column) to characterize the product distribution. Hydrogenation of the oligomeric fuels leads to the elimination of stereoisomers and therefore enables the determination of the degree of branching. According to the procedure described by Heveling et al. [41], the liquid product is mixed with a commercial hydrogenation catalyst (10 wt % Pd/C, Sigma-Aldrich) and is hydrogenated at 80 °C and 30 bar hydrogen pressure in a stainless-steel autoclave.

3 Results and Discussion

3.1 Influence of Feed Composition on (Co-)Oligomerization

Different olefin feedstocks were investigated within this study. Within all experiments, a pseudo-stationary state with almost constant activity is reached after around 2 h. Conversions are measured after 4 h TOS and the liquid phase is analyzed after 6 h TOS. Results from pure 1-butylene oligomerization are depicted in Fig. 4 and can serve as a reference. In addition, the product distributions of the co-oligomerization of propylene and 1-butylene in a molar ratio of 50:50 and the co-oligomerization of a typical MTO product mixture consisting of 40 mol % ethylene, 40 mol % propylene and 20 mol % 1-butylene are shown. Since a mildly acidic catalyst is applied and the reaction temperature is rather low (120 °C), the formation of aromatics during oligomerization can be ruled out and only olefins with different chain lengths are formed [42].
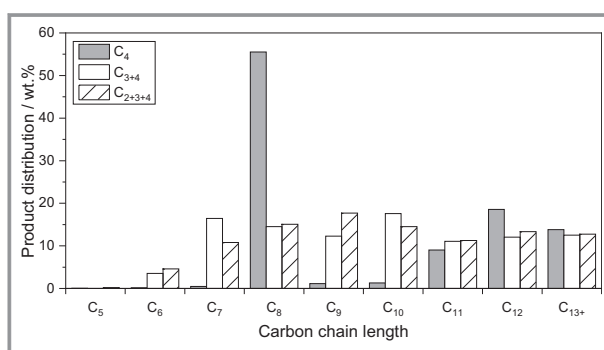

Figure 4. Product distribution for different olefin feedstocks (reaction conditions: T = 120 °C, $p_{Olefins}$ = 32 bar, p_{total} = 40 bar, *WHSV* = 4 h^{-1}).

With only one olefin as feed, a high selectivity to specific chain lengths is achievable. In the case of 1-butylene (XC4 = 86.0 %), primarily integer multiples viz. C$_8$ (proportion of about 55 wt %) and C$_{12}$ (proportion of about 20 wt %) oligomers, as well as C$_{16}$ tetramers (proportion of about 10 wt %) are formed. Due to side reactions such as metathesis or cracking reactions, non-integer multiples, such as C$_{10}$ or C$_{11}$ hydrocarbons, are also formed. Conspicuous is the high selectivity to C$_8$ isomers, which is due to dimerization and forms almost exclusively the gasoline fraction. Higher oligomers up to C$_{16}$ hydrocarbons fit within the typical chain length range of jet fuel. A small proportion of long-chain byproducts C$_{17+}$ with less than 5 wt % is also formed, which is applicable as diesel fuel.

As soon as several olefins are used as feed, product mixtures change considerably. In the case of the co-oligomerization of propylene and 1-butylene, this effect is already apparent, since the maximum proportion of oligomers with a single chain length is drastically reduced from 55 wt % to

about 18 wt %. In general, a homogeneously distributed mixture of oligomers with chain lengths between C_7 and C_{12} is obtained. This can be attributed to the increased number of possible oligomerization routes. Thus, not only the integer multiples of the respective monomers occur but also oligomers stemming from reactions between both reactants, i.e., true co-oligomerization takes place. Consequently, co-oligomers such as C_7 and C_{10} hydrocarbons are obtained in larger proportions. This behavior is also evident in the co-oligomerization of the MTO product mixture. Regarding the chain length of the oligomers, the product spectrum comprises hydrocarbons in the range of gasoline as well as hydrocarbons in the range of jet fuel. The overall selectivity to the gasoline and jet fuel fraction in all experiments is above 90 % and only the proportion of specific chain lengths changes. This offers the possibility of tuning the product distributions and directing them to the desired product fractions.

Regarding the octane number of gasoline, branching of the octenes is important. Linear molecules need to be avoided whereas highly branched hydrocarbons are beneficial and triple-branched octenes offer high RONs around 100. Fig. 5a shows exemplarily the proportion of isomers for different carbon chain lengths. From the C_8 fraction on, the proportion of isomers is above 90 % and varies only slightly.

For the C_6 fraction, the largest differences are visible. In the case of pure 1-butylene oligomerization, C_6 hydrocarbons are produced in small amounts and exclusively by cracking or metathesis reactions. By co-oligomerization of propylene and 1-butylene, hexene is primarily formed by the dimerization of propylene. Since propylene also oligomerizes at acidic centers where isomerization reactions occur, the highest proportion of isomers is formed. In the case of the co-oligomerizations, addition of ethylene reduces the proportion of C_6 isomers. This is due to nickel-catalyzed oligomerization of ethylene, which produces mainly linear molecules [17, 32, 43]. The formation of linear hexenes is also related to the formation of unbranched C_{10}

or C_{12} hydrocarbons, which can be formed by co-oligomerization of linear hexene with 1-butylene or dimerization.

In Fig. 5b, branching within the C_8 fraction is illustrated. Obviously, the olefin feed has only a minor effect on the degree of branching. With about 80 wt % in every experiment, the highest share of C_8 oligomers is double-branched. As described in a previous study [13], the ratio of 2- to 1-butylenes reaches the thermodynamic equilibrium at 120 °C resulting in high shares of 2-butylene and consequently leading to double-branched octenes. Linear and mono-branched octenes are formed with a content of about 10 %, respectively. Regarding their octane numbers, suitability for applications in spark-ignition engines is limited. As already mentioned above, triple-branched isomers would be ideal in terms of octane number, but their content is less than 2 wt % in all experiments. According to [7], double-branched C_8 oligomers exhibit octane numbers in the range of 70–80 and, as shown by Dagle et al. [44], they can be added as blending components in proportions of up to 20 wt % without reducing the RON and the overall quality of the fuel. In addition, the blending offers advantages in terms of improved engine efficiency and reduced soot emissions.

3.2 Influence of Pressure on (Co-)Oligomerization

There are contradictory reports in the literature about the influence of pressure on olefin oligomerization. The effect on the product mixture from the co-oligomerization of an olefin feed mixture has been scarcely investigated yet. Therefore, this aspect has been addressed and results concerning olefin conversion, product composition and branching are described in the following for the same olefin mixtures as in the previous chapter as well as pure propylene.

High pressure is beneficial for the production of liquid products from gases, and this is reflected by the experimental results. Doubling the propylene partial pressure from 16 to 32 bar results in an increase in propylene conversion X_{C3} of almost 40 % from 65.1 to 90.8 %. This behavior is also evident in the co-oligomerization of C_{3+4} and the MTO product mixture (C_{2+3+4}), as shown in Tab. 2. In the latter case, the primary product of ethylene oligomerization at low pressure is butylene [13] disguising the conversion of the originally fed butylene. Particularly at 16 bar, this effect plays an important role as the proportion of butylene in the product stream is high, resulting in a significant drop of its conversion ($X_{C4} = 7.5$ %). In contrast, at 32 bar butylene formation from ethylene is less pronounced due to a higher degree of ethylene oligomerization resulting in higher oligomers.
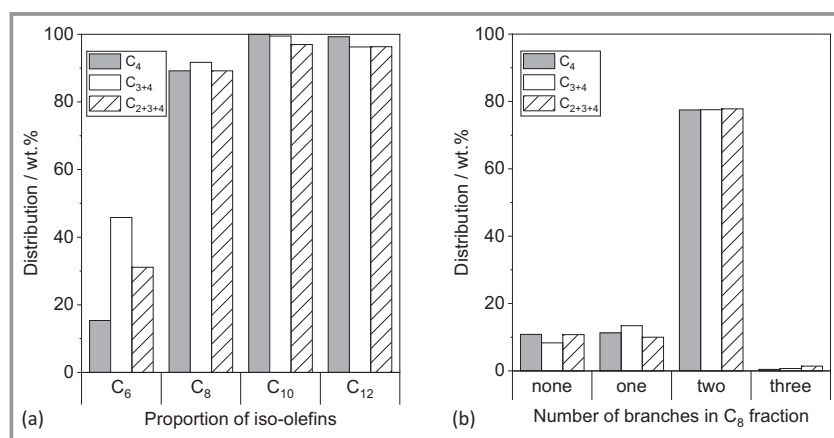

Figure 5. a) Proportion of branched olefins and b) nature of octene isomers for different olefin feedstocks (reaction conditions: $T = 120$ °C, $p_{Olefins} = 32$ bar, $p_{total} = 40$ bar, $WHSV = 4 \, h^{-1}$).

Table 2. Conversion of different olefin feedstocks at 16 and 32 bar olefin partial pressure (p_{total} = 20 and 40 bar, respectively).

Olefin feedstock	C_3		C_{3+4}		C_{2+3+4}	
Olefin partial pressure [bar]	16	32	16	32	16	32
Ethylene conversion X_{C2} [%]					85.4	100
Propylene conversion X_{C3} [%]	65.1	90.8	54.6	88.5	48.8	85.8
Butylene conversion X_{C4} [%]			40.4	66.7	7.5	46.7

Considering the product mixture, propylene oligomerization shows a shift towards smaller oligomers with higher pressure, which is also described for butylene oligomerization in previous studies [26, 34, 35]. For the C_9 trimer, this shift is clearly visible in Fig. 6 as the C_9 content increases by about 50 % while increasing the partial pressure from 16 bar to 32 bar. Hexenes are present only to a minor extent in the liquid product fraction. Thus, hexenes appear to be only intermediates for further oligomerization steps to higher oligomers. Regarding the pressure dependence in the case of co-oligomerization, product distributions are only slightly dependent on pressure and the trend towards shorter chain lengths is less pronounced at higher pressures. However, regarding the C_{13+} fraction, its content is significantly lower at 32 bar olefin partial pressure than at 16 bar. The reduction is around 20 % in the case of C_{3+4} oligomerization and around 30 % in the case of C_{2+3+4} oligomerization. This overall shift in product distribution may be attributed to the increased presence of liquid hydrocarbons and consequently to mass transfer limitations as proposed by Díaz et al. [26]. At 32 bar and 120 °C, more liquid products are obtained compared to 16 bar, which is due to increased olefin conversion. Consequently, pores with the catalyst's active sites may get occupied by liquids to a larger extent. Thus, diffusion of gaseous educts to the active sites of the catalysts is more hindered than at lower operating pressures with lower proportions of liquid oligomers. Additionally, liquid products may also serve as a solvent, promoting the desorption of the oligomers and therefore, reducing their residence time on active sites. As a result, lower degrees of oligomerization are achieved leading to the observed shifts in the product distributions.
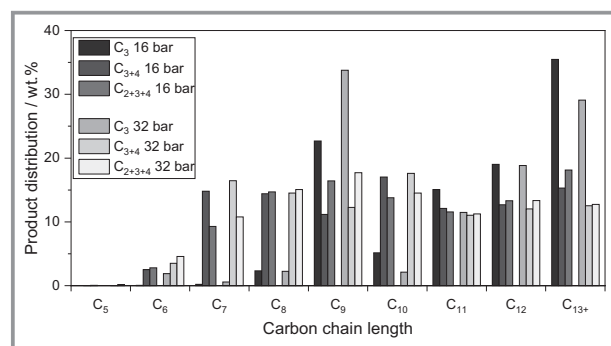
The product distribution at 16 bar shows higher proportions of C_{13+} oligomers than at 32 bar. Larger oligomers lead to olefin confinement in the catalyst pores and the formation of coke. Consequently, the catalyst deactivates due to pore blockage. An investigation of catalyst deactivation after 24 h TOS showed that by heating the reactor to 300 °C for 8 h under 200 mL min^{-1} argon flow, the initial activity of the catalyst was restored. This can be attributed to the formation of soft coke, which desorbs from the catalyst surface at elevated temperatures [45]. As a result, higher pressure allows the catalyst to operate longer before regeneration due to a reduced share of higher olefins and thus, less coke formation and catalyst deactivation.

Concerning the branching of the liquid products, pressure variation exhibits a low impact. In the (co-)oligomerization experiments, only minor changes in the proportion of iso-olefins (Fig. 7a) and the degree of branching in the octene fraction (Fig. 7b) occur. At 32 bar, only 38 % of the hexenes are branched due to the formation of linear hexenes via propylene dimerization on nickel sites [11]. However, propylene oligomerization leads to proportions of C_9 isomers exceeding 97 % in both experiments (not shown in Fig. 7a). Consequently, the acid-catalyzed oligomerization of linear hexenes with propylene leads almost exclusively to branched C_9 isomers and ultimately the differences in isomer proportions of C_6 and C_9. In the co-oligomerization experiments, this effect is also evident as the proportion of C_9 iso-olefins is always above 96 %, whereas the proportion of C_6 iso-olefins is less than 50 %. Concerning the number of branches in the C_8 fraction, the highest proportions are double-branched. During propylene oligomerization, C_8 oligomers are formed exclusively at acid sites by metathesis or cracking reactions, resulting in branched hydrocarbons. The pressure levels do not significantly change the degree of molecular branching. Consequently, the acid-catalyzed reactions appear to be largely independent of pressure.

4 Conclusion

Olefins exhibit a great potential to become a key component for the production of renewable fuels. The present study shows that the heterogeneously catalyzed oligomerization of methanol-based olefins is a promising option for the supply of fuels for gasoline or jet fuel applications. Various olefin mixtures consisting of ethylene, propylene and 1-butylene were converted at different olefin partial pressures and product distributions including the branching of the oligomers were determined. The results enable identification of preferred reaction pathways and beneficial operating conditions for olefin (co-)oligomerization on silica-alumina
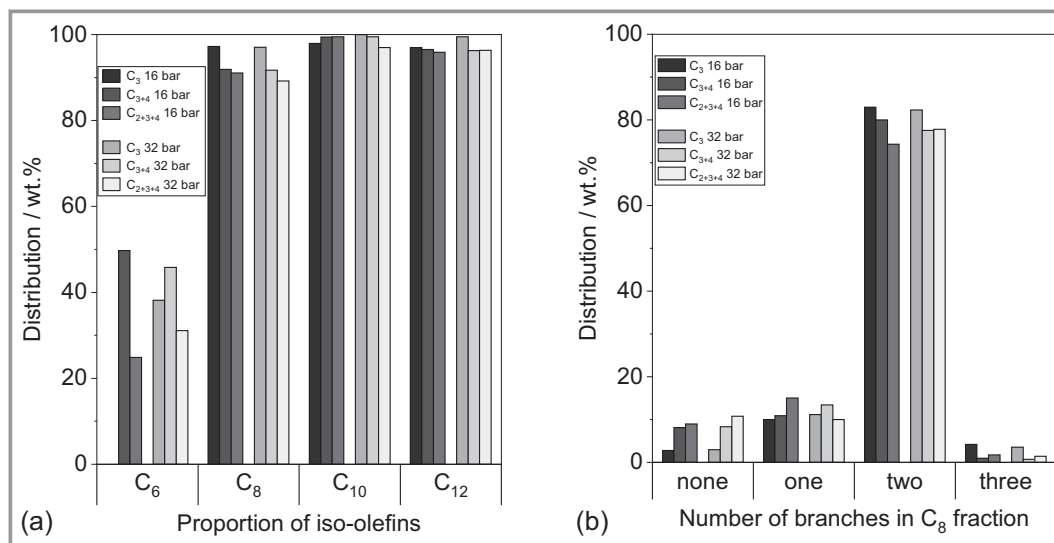

Figure 6. Product distribution for different olefin feedstocks at $p_{Olefins}$ = 16 bar and $p_{Olefins}$ = 32 bar (reaction conditions: T = 120 °C, $WHSV$ = 4 h^{-1}).

Figure 7. a) Proportion of branched olefins and b) nature of octene isomers for different olefin feedstocks and partial pressures (reaction conditions: $T = 120\,°C$, $WHSV = 4\,h^{-1}$).

supported nickel catalysts. The olefin feedstock strongly influences the product distribution enabling a tunable process for the production of specific fuel fractions. With different olefins as educts, co-oligomerization leads to more evenly distributed product mixtures with an overall selectivity above 90 % to C_{5-16} hydrocarbons, i.e., gasoline and jet fuel.

Varying the olefin partial pressure of the employed olefin feed mixtures only marginally affects the degree of oligomerization of the products by shifting it towards smaller oligomers. The formation of soft coke on the catalyst is reduced at elevated pressure, which extends the operating time until catalyst regeneration is required. Branching and isomerization are only slightly dependent on the applied pressure, but the results enable to conclude on reaction pathways to higher oligomers. It could be shown that at higher pressure linear hexenes, produced by nickel-catalyzed oligomerization of ethylene or propylene, react with propylene on acid sites to form almost exclusively branched nonenes. Additionally, olefin conversion increases significantly with increasing pressure resulting in higher yields of liquid products if unconverted olefins are not recycled within the process.

Overall, the produced fuels are free of aromatics and can be synthesized on a renewable basis, which represents a low-emission option for extending the operation of currently existing fleets throughout the transportation sector. In addition, the conventional fuel distribution and tank infrastructure can still be used. A requirement for sustainable and overall low-emission production on large scale is the availability of renewable energies and feedstocks such as methanol and DME. This requirement is currently the dominating challenge for application on commercial scale.

Acknowledgment

Symbols used

C_y	[–]	olefin with y carbon atoms
d_{Pore}	[nm]	pore diameter
p	[bar]	pressure
S_{BET}	[m^{2}g^{-1}]	specific surface
T	[°C]	temperature
V_{Pore}	[mL]	pore volume
$WHSV$	[h^{-1}]	weight hourly space velocity
X_{Cy}	[%]	conversion of olefin with y carbon atoms

Abbreviations

BET	Brunauer-Emmett-Teller
DME	dimethyl ether
DTO	DME to olefins
MTO	methanol to olefins
RON	research octane number
TOS	time on stream

References

[1] IRENA and Methanol Institute, *Innovation outlook, Renewable methanol*, International Renewable Energy Agency, Abu Dhabi **2021**.

[2] T. Cordero-Lanzac, A. T. Aguayo, A. G. Gayubo, J. Bilbao, *Chem. Eng. J.* **2021**, *405*, 126448. DOI: https://doi.org/10.1016/j.cej.2020.126448

[3] S. Xu, Y. Zhi, J. Han, W. Zhang, X. Wu, T. Sun, Y. Wei, Z. Liu, *Adv. Catal.* **2017**, *61*, 37–122. DOI: https://doi.org/10.1016/bs.acat.2017.10.002

[4] T. Cordero-Lanzac, A. Ateka, P. Pérez-Uriarte, P. Castaño, A. T. Aguayo, J. Bilbao, *Ind. Eng. Chem. Res.* **2018**, *57 (41)*, 13689–13702. DOI: https://doi.org/10.1021/acs.iecr.8b03308

[5] P. Eckert, S. Rakowski, in *Grundlagen Verbrennungsmotoren* (Eds: G. P. Merker, R. Teichmann), Vol. 42, Springer Fachmedien Wiesbaden GmbH, Wiesbaden **2019**, 943–977.

[6] DIN EN 228:2012+A1, *Kraftstoffe – Unverbleite Ottokraftstoffe – Anforderungen und Prüfverfahren*, Beuth Verlag GmbH, Berlin **2017**.

[7] STP225-EB, *Knocking Characteristics of Pure Hydrocarbons*, ASTM International, West Conshohocken, PA **1958**.

[8] M. Boltz, P. Losch, B. Louis, *Adv. Chem. Lett.* **2013**, *1 (3)*, 247–256. DOI: https://doi.org/10.1166/acl.2013.1032

[9] M. Bjørgen, F. Joensen, K.-P. Lillerud, U. Olsbye, S. Svelle, *Catal. Today* **2009**, *142 (1–2)*, 90–97. DOI: https://doi.org/10.1016/j.cattod.2009.01.015

[10] D. Chen, K. Moljord, A. Holmen, *Microporous Mesoporous Mater.* **2012**, *164*, 239–250. DOI: https://doi.org/10.1016/j.micromeso.2012.06.046

[11] H. Olivier-Bourbigou, P. A. R. Breuil, L. Magna, T. Michel, M. F. Espada Pastor, D. Delcroix, *Chem. Rev.* **2020**, *120 (15)*, 7919–7983. DOI: https://doi.org/10.1021/acs.chemrev.0c00076

[12] E. Koninckx, P. S. Mendes, J. W. Thybaut, L. J. Broadbelt, *Appl. Catal., A* **2021**, *624*, 118296. DOI: https://doi.org/10.1016/j.apcata.2021.118296

[13] M. Betz, C. Fuchs, T. A. Zevaco, U. Arnold, J. Sauer, *Biomass Bioenergy* **2022**, *166*, 106595. DOI: https://doi.org/10.1016/j.biombioe.2022.106595

[14] P. Liu, E. Redekop, X. Gao, W.-C. Liu, U. Olsbye, G. A. Somorjai, *J. Am. Chem. Soc.* **2019**, *141 (29)*, 11557–11564. DOI: https://doi.org/10.1021/jacs.9b03867

[15] C. T. O'Connor, in *Handbook of Heterogeneous Catalysis* (Ed: G. Ertl), 2. Ed., Wiley-VCH, Weinheim **2008**.

[16] C. P. Nicholas, *Appl. Catal., A* **2017**, *543*, 82–97. DOI: https://doi.org/10.1016/j.apcata.2017.06.011

[17] C. Fuchs, U. Arnold, J. Sauer, *Chem. Ing. Tech.* **2022**, *94 (9)*, 1215. DOI: https://doi.org/10.1002/cite.202255176

[18] H. Shao, H. Li, J. Lin, T. Jiang, X. Guo, J. Li, *Eur. Polym. J.* **2014**, *59*, 208–217. DOI: https://doi.org/10.1016/j.eurpolymj.2014.08.002

[19] D. S. McGuinness, *Chem. Rev.* **2011**, *111 (3)*, 2321–2341. DOI: https://doi.org/10.1021/cr100217q

[20] L. H. Do, J. A. Labinger, J. E. Bercaw, *Organometallics* **2012**, *31 (14)*, 5143–5149. DOI: https://doi.org/10.1021/om300492r

[21] R. G. Da Rosa, M. O. de Souza, R. F. de Souza, *J. Mol. Catal. A: Chem.* **1997**, *120 (1–3)*, 55–62. DOI: https://doi.org/10.1016/S1381-1169(96)00438-4

[22] P. A. R. Breuil, L. Magna, H. Olivier-Bourbigou, *Catal. Lett.* **2015**, *145 (1)*, 173–192. DOI: https://doi.org/10.1007/s10562-014-1451-x

[23] W. Monama, E. Mohiuddin, B. Thangaraj, M. M. Mdleleni, D. Key, *Catal. Today* **2020**, *342*, 167–177. DOI: https://doi.org/10.1016/j.cattod.2019.02.061

[24] S. A. Tabak, S. Yurchak, *Catal. Today* **1990**, *6 (3)*, 307–327. DOI: https://doi.org/10.1016/0920-5861(90)85007-b

[25] A. Ehrmaier, Y. Liu, S. Peitz, A. Jentys, Y.-H. C. Chin, M. Sanchez-Sanchez, R. Bermejo-Deval, J. Lercher, *ACS Catal.* **2019**, *9 (1)*, 315–324. DOI: https://doi.org/10.1021/acscatal.8b03095

[26] M. Díaz, E. Epelde, Z. Tabernilla, A. Ateka, A. T. Aguayo, J. Bilbao, *Energy* **2020**, *207*, 118317. DOI: https://doi.org/10.1016/j.energy.2020.118317

[27] C. Fuchs, M. Betz, U. Arnold, J. Sauer, in *13th International Colloquium Fuels*, Conventional and Future Energy for Automobiles, 1. Ed., expert, Tübingen **2021**.

[28] B. H. Babu, M. Lee, D. W. Hwang, Y. Kim, H.-J. Chae, *Appl. Catal., A* **2017**, *530*, 48–55. DOI: https://doi.org/10.1016/j.apcata.2016.11.020

[29] B. M. Antunes, A. E. Rodrigues, Z. Lin, I. Portugal, C. M. Silva, *Fuel Process. Technol.* **2015**, *138*, 86–99. DOI: https://doi.org/10.1016/j.fuproc.2015.04.031

[30] E. Kriván, S. Tomasek, J. Hancsók, *J. Cleaner Prod.* **2016**, *136*, 81–88. DOI: https://doi.org/10.1016/j.jclepro.2016.06.020

[31] M. Lee, J. W. Yoon, Y. Kim, J. S. Yoon, H.-J. Chae, Y.-H. Han, D. W. Hwang, *Appl. Catal., A* **2018**, *562*, 87–93. DOI: https://doi.org/10.1016/j.apcata.2018.06.004

[32] F. Nadolny, F. Alscher, S. Peitz, E. Borovinskaya, R. Franke, W. Reschetilowski, *Catalysts* **2020**, *10 (12)*, 1487. DOI: https://doi.org/10.3390/catal10121487

[33] S. Forget, H. Olivier-Bourbigou, D. Delcroix, *ChemCatChem* **2017**, *9 (12)*, 2408–2417. DOI: https://doi.org/10.1002/cctc.201700348

[34] O. Jan, F. L. Resende, *Fuel Process. Technol.* **2018**, *179*, 269–276. DOI: https://doi.org/10.1016/j.fuproc.2018.07.004

[35] A. F. Silva, A. Fernandes, M. M. Antunes, P. Neves, S. M. Rocha, M. F. Ribeiro, M. Pillinger, J. Ribeiro, C. M. Silva, A. A. Valente, *Fuel* **2017**, *209*, 371–382. DOI: https://doi.org/10.1016/j.fuel.2017.08.017

[36] A. F. Silva, A. Fernandes, P. Neves, M. M. Antunes, S. M. Rocha, M. F. Ribeiro, C. M. Silva, A. A. Valente, *ChemCatChem* **2018**, *10 (13)*, 2741–2754. DOI: https://doi.org/10.1002/cctc.201701597

[37] D. York, J. Scheckler, D. Tajbl, in *Handbook of Petroleum Refining Processes* (Ed: R. A. Meyers), McGraw-Hill, New York **1997**, Ch. 1–3.

[38] V. N. Ipatieff, B. B. Corson, G. Egloff, *Ind. Eng. Chem.* **1935**, *27 (9)*, 1077–1081. DOI: https://doi.org/10.1021/ie50309a027

[39] S. A. Tabak, F. J. Krambeck, *Hydrocarbon Process.* **1985**, *64 (9)*, 72–74.

[40] *Doped Aluminas – Silica-Aluminas Mixed Metal Oxides*, Sasol Performance Chemicals, Hamburg. www.sasolgermany.de/fileadmin/doc/alumina/0271.SAS-BR-Inorganics_Siral_Siralox_WEB.pdf (Accessed on November 03, 2022)

[41] J. Heveling, C. P. Nicolaides, M. S. Scurrell, *Appl. Catal., A* **1998**, *173 (1)*, 1–9. DOI: https://doi.org/10.1016/S0926-860X(98)00147-1

[42] A. V. Lavrenov, T. R. Karpova, E. A. Buluchevskii, E. N. Bogdanets, *Catal. Ind.* **2016**, *8 (4)*, 316–327. DOI: https://doi.org/10.1134/S2070050416040061

[43] S. Albrecht, D. Kießling, G. Wendt, D. Maschmeyer, F. Nierlich, *Chem. Ing. Tech.* **2005**, *77 (6)*, 695–709. DOI: https://doi.org/10.1002/cite.200407090

[44] V. L. Dagle, M. Affandy, J. S. Lopez, L. Cosimbescu, D. J. Gaspar, S. Scott Goldsborough, T. Rockstroh, S. Cheng, T. Han, C. P. Kolodziej, A. Hoth, S. S. Majumdar, J. A. Pihl, T. L. Alleman, C. Hays, C. S. McEnally, J. Zhu, L. D. Pfefferle, *Fuel* **2022**, *310*, 122314. DOI: https://doi.org/10.1016/j.fuel.2021.122314

[45] M. Díaz, E. Epelde, J. Valecillos, S. Izaddoust, A. T. Aguayo, J. Bilbao, *Appl. Catal., B* **2021**, *291*, 120076. DOI: https://doi.org/10.1016/j.apcatb.2021.120076